COBISS: 1.01

ISOTOPES OF CARBON IN A KARST AQUIFER OF THE CUMBERLAND PLATEAU OF KENTUCKY, USA

OGLJIKOVI IZOTOPI V KRAŠKEM VODONOSNIKU CUMBERLANDSKE PLANOTE , KENTUCKY, ZDA

Lee J. FLOREA[1]

Abstract UDC UDK: 546.26.027*14:551.444(736.9)

Lee J. Florea: Isotopes of Carbon in a Karst Aquifer of the Cumberland Plateau of Kentucky, USA

In this study, the concentration and isotopic composition of dissolved organic carbon (DOC) and dissolved inorganic carbon (DIC) are measured in the karst groundwater of the Otter Creek watershed of the Cumberland Plateau of Kentucky, USA. Comparisons among these data and with the geochemistry of carbonate and gypsum equilibrium reactions reveal that DOC concentration is inversely related to discharge, multiple reaction pathways provide DIC with isotopic enrichment that may be directly related to mineral saturation, and oxidation of reduced sulfur is possible for dissolution. DOC is derived from C3 vegetation with an average $\delta^{13}C_{DOC}$ of −27‰. DIC in groundwater is derived from both pedogenic CO_2 and HCO_3^- from dissolved carbonate. At input sites to the karst aquifers DIC concentrations are expectedly low, less than 1 mmol/L, in waters that are undersaturated with respect to calcite. At the output of these karst aquifers DIC concentrations reach 3 mmol/L in waters that are at or above calcite saturation. Values of $\delta^{13}C_{DIC}$ range between −6.3 and −12.4‰ with CO_2 degassing and calcite precipitation at some sites obfuscating a simple relationship between $\delta^{13}C_{DIC}$, discharge, and mineral saturation. In addition, concentrations of DIC in sulfur seeps within the watershed range between 2–7 mmol/L with $\delta^{13}C_{DIC}$ values in some samples skewed more toward the anticipated value of carbonate bedrock than would be expected from reactions with carbonic acid alone. This suggests that the oxidation of reduced sulfur from shallow oilfield brines liberates bedrock DIC through reactions with sulfuric acid.

Keywords: dissolved organic carbon, dissolved inorganic carbon, sulfur redox, ion geochemistry, saturation index.

Izvleček UDK UDK: 546.26.027*14:551.444(736.9)

Lee J. Florea: Ogljikovi izotopi v kraškem vodonosniku Cumberlandske planote, Kentucky, ZDA

V kraški podtalnici zaledja potoka Otter Creek (Cumberlandska planota, Kentucky, ZDA), smo merili koncentracijo in izotopsko sestavo raztopljenega organskega (DOC) in anorganskega (DIC) ogljika. Podatke smo primerjali z ravnotežno kemijo karbonatov in sadre. Ugotovili smo, da koncentracija DOC pada s pretokom vode, da lahko izotopsko obogatitev DIC vzdolž več reakcijskih poti, neposredno povežemo z nasičenostjo raztopine in da ima pri raztapljanju pomembno vlogo oksidacija reduciranega žvepla. DOC izhaja iz vegetacije tipa C3, s povprečno $\delta^{13}C_{DOC}$ −27‰. DIC izhaja iz pedogenega CO_2 in iz raztopljenih karbonatov v obliki HCO_3^- . Dotoki v vodonosnik so nenasičeni na kalcit in imajo izrazito nizk koncentracijo DIC, manj kot 1 mmol/L. Na izvirih so vode v ravnotežju oz. prenasičene na kalcit, koncentracija DIC pa doseže 3 mmol/L. Na mestih, kjer iz vode izhaja CO_2 in se izloča kalcit, so izotopske vrednosti DIC med −6,3 in −12,4 ‰, kar zamegljuje enostavna razmerja med $\delta^{13}C_{DIC}$, pretokom in stopnjo nasičenja. V žveplenih vodah so koncentracije DIC med 2–7 mmol/L in odstopajo od vrednosti, ki bi jih pričakovali pri raztapljanju karbonatov z ogljikovo kislino, v smeri vrednosti v matični karbonatni kamnini. Očitno se del DIC iz karbonatov sprošča pri reakciji z žvepleno kislino, ki nastaja ob oksidaciji reduciranega žvepla iz plitvih slanic naftnih polj.

Ključne besede: raztopjen organski in anorganski ogljik, redukcija žvepla, geokemija, indeks nasičenja.

[1] Department of Geological Sciences, Ball State University, e-mail: lflorea@bsu.edu

Received/Prejeto: 25.2.2013

INTRODUCTION

Carbonate aquifers, hosting 60% of the world's proven petroleum reservoirs, 40% of known gas reserves, and influencing approximately 25% of the world's drinking water (Ford and Williams 2007), are particularly vital to our understanding of the global carbon cycle. A significant fraction of carbon transport through karst is in dissolved form. Dissolved organic carbon (DOC) comprises organic acids and carbohydrates leached out of vegetation and soil. The composition of that DOC depends largely upon the overlying climate and land use. Dissolved inorganic carbon (DIC) includes products of mineral reactions with acidity in water. Of primary importance is the carbonate equilibrium reaction with calcite and dolomite, or

$$H_2CO_{3(aq)} + [(1-x)Ca, xMg]CO_{3(sol)} \leftrightarrow (1-x)Ca_{(aq)} + xMg_{(aq)} + 2HCO_{3(aq)}, \quad (1)$$

where the subscripts x and 1-x are proportional to the magnitude of calcite and dolomite within a karst aquifer, respectively. In *Equation 1*, CO_2 sequestered into the aqueous system from the atmosphere, organic oxidation, or microbial respiration in the soil reacts with carbonate bedrock to release carbonate ions into solution. In the pH ranges typical of water in karst aquifers, bicarbonate (HCO_3^-) is the principal dissolved ion.

More recently, some emphasis has shifted toward carbonate aquifers with secondary porosity that has partly evolved via the oxidation of reduced sulfur, via the following reaction:

$$H_2SO_{4(aq)} + 2[(1-x)Ca, xMg]CO_{3(sol)} \leftrightarrow 2(1-x)Ca_{(aq)} + 2xMg_{(aq)} + SO_{4(aq)} + 2HCO_{3(aq)}. \quad (2)$$

In such systems, such as the classic example of the karst of the Guadalupe Mountains of New Mexico (Hill 1990), CO_2 is not sequestered from the atmosphere and DIC is liberated from the carbonate bedrock alone.

STABLE ISOTOPES OF CARBON

In nature, carbon occurs as two stable isotopes, ^{12}C and ^{13}C with the abundance of the heavier isotope of approximately 1.1%. Mass-spectrometry can distinguish between these isotopes and compute the enrichment or depletion of the heavier isotope of carbon in a sample as compared the Vienna Pee Dee Belemnite (VPDB), denoted by $\delta^{13}C$ and calculated using

$$\delta^{13}C = \frac{^{13}C / ^{12}C_{(sample)} - ^{13}C / ^{12}C_{(VPDB)}}{^{13}C / ^{12}C_{(VPDB)}} \times 1000. \quad (3)$$

Values of $\delta^{13}C$ are reported in parts per thousand or 'per mille' (‰ – VPDB). Various processes in nature may fractionate the heavier or lighter stable isotope of carbon (Kendall & Caldwell 1998)

In vegetation, the photosynthetic process preferentially uptakes the lighter isotope during carbon fixation (Schlesinger 1997; Ehleringer & Cerling 2000). The resulting $\delta^{13}C$ of organic carbon in vegetation is depleted in the heavier isotope. The magnitude of this fractionation depends upon the nature of the photosynthetic pathway. In humid landscapes, most native plants utilize the C3 pathway, which yields organic matter with $\delta^{13}C$ values between -23 and -27‰. C4-type vegetation, in contrast, is more adapted to arid conditions, fixes less CO_2 during photosynthesis than the C3 pathway, and consequently has $\delta^{13}C$ values between -10 and -14‰.

In shallow ground water, values of $\delta^{13}C$ in dissolved organic and inorganic carbon ($\delta^{13}C_{DOC}$ and $\delta^{13}C_{DIC}$) reflect a combination of microbiologic reactions, limestone dissolution, and gas-water exchange processes. When carbon dioxide CO_2 produced in soil by oxidation or by biogenic reactions is dissolved into water, the process preferentially selects the heavier isotope. The $\delta^{13}C_{DIC}$ resulting enrichment is from combined microbial, diffusion, and equilibrium fractionation and may be as much as +6.4‰ (Clark & Fritz 1997). This pedogenic-derived DIC reacts with carbonate bedrock via *Equation 1* to produce a DIC in groundwater from each source, with the stoichiometry in a simple reaction mandating a 50% blend of carbon in the products at mineral saturation. Undersaturated solutions would theoretically have values of $\delta^{13}C_{DIC}$ that more reflect soil CO_2. Oversaturated solutions may be more enriched in bedrock-derived DIC compared to a sample at saturation.

The exact nature of $\delta^{13}C_{DIC}$ in karst groundwater can be significantly more complex than simple mixing and governed by phases of CO_2 enrichment or degassing along the flowpath (Marlier & O'Leary 1984), by alternative chemical weathering phenomena like those that release DIC from carbonate bedrock into an aqueous solution without corresponding soil CO_2 (e.g., *Equation 2*), or by weathering of certain silicates that sequesters CO_2 from the atmosphere without the addition of bedrock DIC (e.g., weathering of wollastinite, $CaSiO_3$ – Berner *et al.* 1983). In summary, changes in end-member contributions to DOC and DIC (e.g., vegetative cover and bedrock composition) as well as variations in the hydraulic function of the underlying aquifer system from droughts or storm events may manifest as changes to the values of $\delta^{13}C_{DIC}$.

This paper considers the spatial and temporal variation of dissolved organic and inorganic carbon from one portion of the karst within the western margin of the Cumberland Plateau in southeast Kentucky as a component of a larger-scale investigation of carbon flux from karst in the Appalachian lowland plateaus. To that end, the geochemistry of water samples from sites considered by Dugan *et al.* (2012) and Florea (2013a) are used to compute calcite and gypsum saturation indices, calcite saturation ratios, as well as the concentration of the species of inorganic carbon. Complementary to these data are measurements of dissolved organic carbon (DOC) and the stable isotopes of dissolved carbon in both organic and inorganic form ($\delta^{13}C_{DOC}$ and $\delta^{13}C_{DIC}$) in these same samples. Variations in these data are investigated as they pertain to sampling site and aquifer characteristics, as well as seasonal patterns manifest, in part, as variations in discharge at selected sites.

HYDROGEOLOGIC SETTING

Data in this study come from water samples collected within the Otter Creek watershed along the western escarpment of the Cumberland Plateau in Wayne County of southeastern Kentucky, USA (Fig. 1). Otter Creek is a third-order tributary of the Cumberland River. Staged incision of the Cumberland River associated with interglacial phases of Plio-Pleistocene glaciation has been the primary control on the geomorphic evolution of the region (Anthony & Granger 2004) and has resulted in tiered cave systems (Simpson & Florea 2009). These caves have developed within middle-Mississippian carbonates of the Slade Formation, including, from oldest to youngest, the St. Louis, Ste. Genevieve, Kidder, and Bangor Limestone members (Ettensohn *et al.* 1984). These are underlain

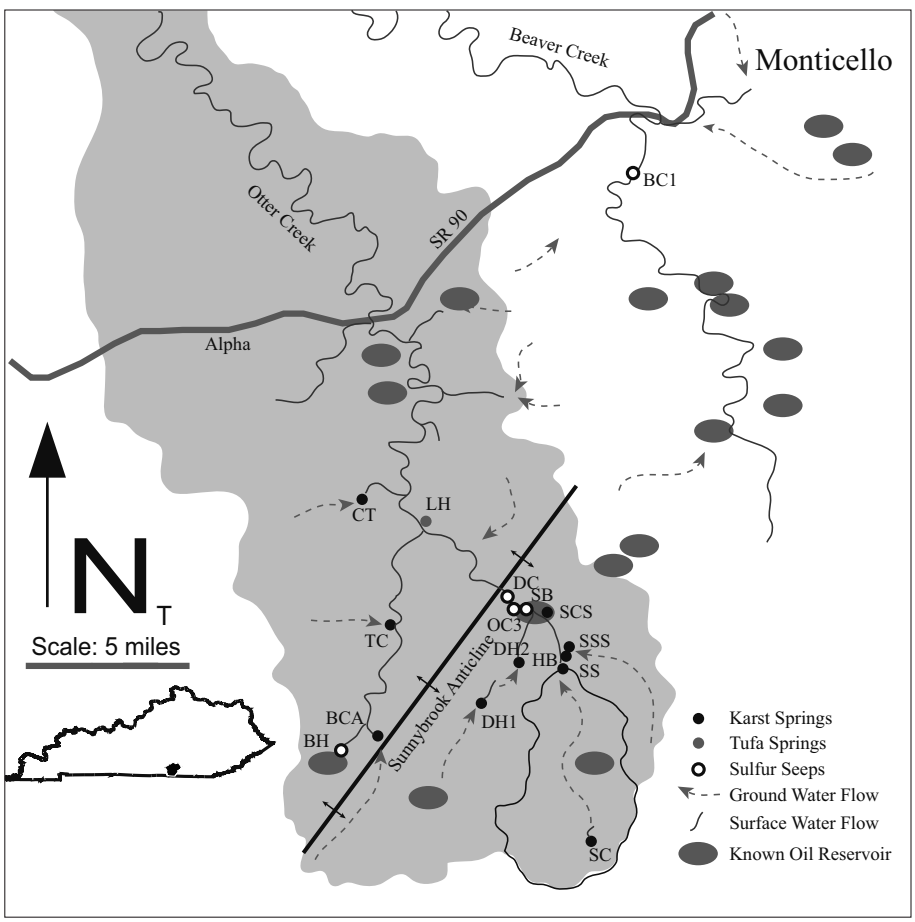

Fig. 1: Study area in Wayne County, KY, USA. Index map of Kentucky illustrates the location of Wayne County. The light gray is the Otter Creek watershed. The Redmond Creek karst aquifer outlined in black includes the sampling sites for Sandy Springs and Stream Cave and are indicated by SS and SC, respectively. Other sampling sites, including karst springs, tufa springs, and sulfur seeps are labled with codes decribed in the text. The axis of the Sunnybrook Anticline is indicated as a black line. Groundwater flow paths are inferred by dye tracing and known cave survey. Oil reservoirs in shallow Mississippian-age strata identified by Abbott (1921) are denoted by gray ovals.

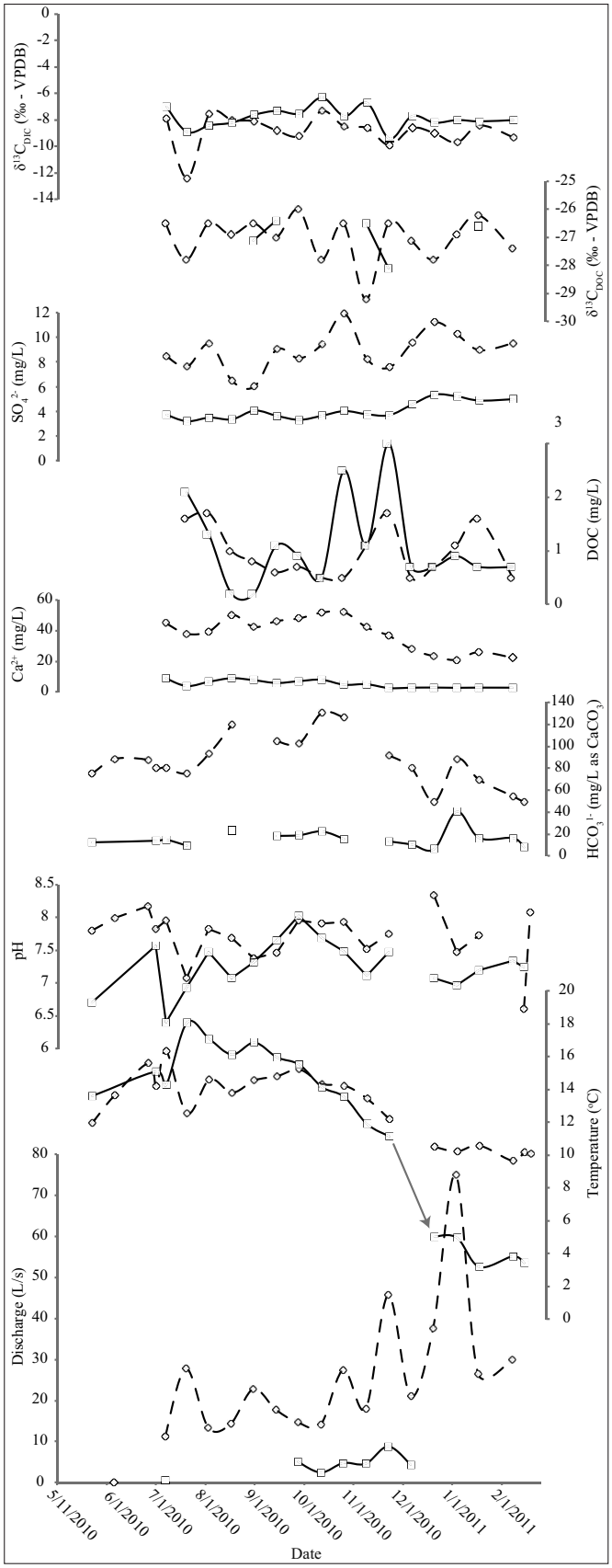

by the early-Mississippian calcareous shale of the Salem-Warsaw and Fort Payne Formations and overlain by the late-Mississippian calcareous shale of the Paragon Formation. Regionally, early Pennsylvanian sandstones and conglomerates of the Lee Formation comprise the plateau surface. Relief in the study area exceeds 230 m with ridge tops above 530 m and valley floors below 300 m.

The active flow system in the karst aquifers of the Otter Creek watershed comprise dendritic networks of tributary conduits (Palmer 1991) that 'stair step' through the stratigraphy (Crawford 1984) and emerge briefly at the land surface where the flowpath at the base of the Bangor Limestone traverses the Hartselle Formation before sinking again into the Kidder Limestone (Walden *et al.* 2007). These tributaries coalesce into sinuous, master conduits that may parallel hillside contours (Sasowsky 1994) and discharge at gravity-flow springs at the base of the plateau (Crawford 1984). The karst of the Cumberland Plateau is largely epigene; in other words, the source of acidity is derived from meteoric recharge and driven largely by the carbonate equilibrium reaction presented in *Equation 1*. Florea (2013b) considers the timing and mode of this recharge using stable isotopes of oxygen and hydrogen ($\delta^{18}O$ and $\delta^{2}H$) and reveals a strong seasonal bias toward winter months when evapotranspiration is reduced.

Fig. 2: Time series plots of selected field, ion, and carbon data from Stream Cave (SC – open squares and solid line) and Sandy Springs (SS – open diamonds and dashed line). All y-axes share the dates at the bottom of the figure.

In addition to the springs from epigene karst aquifers, preliminary geochemical investigations in the Otter Creek watershed by Dugan *et al.* (2012) provide a first look at geochemical data of water chemistry from travertine (tufa) springs and sulfur seeps, that are in part spatially controlled by the Sunnybrook Anticline (Fig. 1). This anticline has an amplitude of approximately 30 m, is oriented N-NE, and is parallel to the trend of the Cumberland Escarpment. Waters at the tufa springs can be oversaturated with respect to calcite and where they emerge, calcite precipitates. These springs probably resurge from long, strike-parallel flowpaths on the west flank of the anticline. Similarly, some caves in the region contain significant travertine deposits within active water passages, including rimstone dams and flowstone, suggesting periods of calcite oversaturation linked with chemical changes that lead to mineral precipitation.

Florea (2013a) investigates the nature of water chemistry in the Otter Creek watershed, in particular from the Redmond Creek karst aquifer (Fig. 1), and using a comparison of reaction products and principal component analysis concludes that, although dissolution via *Equation 1* dominates the chemistry, dissolution via *Equation 2*, with the sulfur derived from the entrainment of shallow brines, is possible at the local scale. This process is particularly important adjacent to sulfur seeps in caves and streams. These documented sulfur seeps are largely concentrated on the east flank of the Sunnybrook Anticline in the direction of the Appalachian Basin (Fig. 1). The presence of these seeps is a manifestation of shallow petroleum reservoirs in lower Mississippian strata that underlie the carbonates that host the karst aquifers (Fig. 2).

METHODS

SAMPLES AND ANALYTICAL METHODS

Samples comprising this study include 16 bi-monthly samples collected in 2010–2011 from two sites in the Redmond Creek karst aquifer, Stream Cave (SC) and Sandy Springs (SS) considered by Florea (2013a and b). Measurements of instantaneous discharge (Q) computed using an acoustic flow meter and standard USGS gauging techniques (e.g., Rantz 1982) accompany these samples. At Stream Cave, water emerges from a hillside spring in the Bangor Limestone, traverses the Hartselle Formation, and sinks within 100 m into the underlying Kidder Limestone. This site represents one of many inputs to the Redmond Creek karst aquifer. Sandy Springs, in contrast, is the principal outlet for the Redmond Creek karst aquifer. Complementing these data are samples collected in 2011 from three sulfur seeps: Slickford Bridge (SB), Bertram Hollow (BH), and Beaver Creek #1 (BC1). In January of 2012, additional samples from 13 springs in the Otter Creek watershed complete the dataset. These samples come from SS, SB, Otter Creek #3 (OC3), Don Carter Seep (DC), Blowing Cave (BCA), Tonya's Cave (TC), Coal Trace (CT), Herlan Buck Springs (HB), Triple S Cave (SSS), Spelunger Cave Springs (SCS), Dry Hollow #1 (DH1), Dry Hollow #2 (DH2), and Light House Spring (LH). Three of these sites (SB, OC3, and DC) represent sulfur seeps. Nine additional sites (SS, BCA, TC, CT, HB, SSS, SCS, DH1, DH2) are classic, gravity-flow karst springs. The remaining site (LH) is a large tufa spring. With the exception of SC, all springs in this study arise from at or near the base of the St. Louis limestone, the regional base of the primary carbonate sequence in the Carboniferous.

Data from the samples are summarized in Tab. 1. These data comprise ionic measurements using HACH field titrations for bicarbonate (HCO_3^-) as well as Ca^{2+} and Mg^{2+} concentrations in the 2012 samples, ion chromatography for 2010–2011 samples, and a HACH DR 2800 spectrophotometer for select ions in the 2012 samples. Field measurements of pH and temperature (T) complement these data. Samples for ion analysis were filtered using a 0.45-μm membrane and collected using 250 mL HDPE bottles and kept at 4°C until time of analysis. Samples for cations were preserved using 2 mL of 6N HNO_3. Precision and accuracy were not reported from the lab contracted for the ion analyses. Computed charge balance values are reported in Tab. 1 for samples where appropriate.

For each filtered sample, a split was stored in a 30-mL glass bottle, treated with $CuSO_4$ as an anti-microbial agent, and stored at 4°C with a parafilm seal until analysis for $\delta^{13}C_{DIC}$. A similar split sample was analyzed for $\delta^{18}O$ and $\delta^{2}H$ with results summarized in Florea (2013b). Concurrent with each of the 16 sets of 2010–2011 data from SC and SS, samples for measurement of DOC and $\delta^{13}C_{DOC}$ were collected in a 1L HDPE bottle spiked with 1 mL of 12 N HCl to prevent microbial activity. In the lab, these samples were dehydrated and the remaining solids treated with H_2SO_3 to effervesce CO_2

Tab. 1. Selected field, ion, and carbon data from sample collection.

Site	Sample Name	Date	Temp	pH	Cations				Anions					Chg Bal	Carbon		
					Ca^{2+}	Mg^{2+}	K^{+}	Na^{+}	HCO_3^{-}	Fl^{-}	Cl^{-}	NO_3^{-}	SO_4^{2-}		DOC	$\delta^{13}C_{DOC}$	$\delta^{13}C_{DIC}$
			(ºC)		mmol/L	mmol/L	mmol/L	mmol/L	mmol/L	mmol/L	mmol/L	mmol/L	mmol/L	%	mg/L	‰ - VPDB	‰ - VPDB
SS	NL070710A	07/07/10	16.33	7.95	1.120	0.225	0.026	0.155	1.61	0.008	0.137	0.053	0.088	18		-26.5	-7.9
SS	NL072010A	07/20/10	12.54	7.08	0.948	0.196	0.024	0.112	1.51	0.008	0.090	0.038	0.079	14	1.6	-27.8	-12.4
SS	NL080310A	08/03/10	14.60	7.82	0.987	0.197	0.024	0.178	1.87	0.008	0.139	0.040	0.099	6	1.7	-26.5	-7.5
SS	NL081710A	08/17/10	13.80	7.69	1.259	0.219	0.026	0.092	2.39	0.008	0.087	0.075	0.067	6	1.0	-26.9	-8.0
SS	NL083110A	08/31//10	14.55	7.38	1.057	0.195	0.023	0.108		0.007	0.081	0.050	0.063		0.8	-26.5	-8.1
SS	NL091410A	09/14/10	14.80	7.46	1.154	0.219	0.024	0.148	2.09	0.007	0.125	0.054	0.094	8	0.6	-27.0	-8.8
SS	NL092810A	09/28/10	15.21	7.95	0.413	0.204	0.002	0.206	2.05	0.003	0.205	0.064	0.086	27	0.7	-26.0	-9.2
SS	NL101210A	10/12/10	14.34	7.91	1.290	0.230	0.024	0.260	2.61	0.004	0.245	0.070	0.098	3	0.5	-27.8	-7.3
SS	NL102610A	10/26/10	14.24	7.93	1.300	0.239	0.025	0.260	2.52	0.004	0.261	0.076	0.124	4	0.5	-26.5	-8.5
SS	NL110910A	11/09/10	13.44	7.52	1.053	0.197	0.024	0.163		0.003	0.154	0.059	0.086		1.1	-29.2	-8.6
SS	NL112310A	11/23/10	12.18	7.75	0.914	0.168	0.025	0.083	1.83	0.004	0.080	0.042	0.079	3	1.7	-26.5	-9.9
SS	NL120710A	12/07/10			0.697	0.136	0.020	0.188	1.61	0.012	0.170	0.032	0.099	4	0.5	-27.1	-8.6
SS	NL122110A	12/21/10	10.50	8.34	0.582	0.113	0.017	0.208	0.99	0.002	0.199	0.041	0.117	5	0.7	-27.8	-9.0
SS	NL010411A	01/04/11	10.22	7.47	0.523	0.104	0.016	0.179	1.77	0.001	0.172	0.030	0.107	20	1.1	-26.9	-9.7
SS	NL011811A	01/18/11	10.58	7.73	0.651	0.151	0.016	0.113	1.39	0.002	0.099	0.022	0.093	1	1.6	-26.2	-8.4
SS	NL020811A	02/08/11	9.64		0.557	0.135	0.015	0.130	1.09	0.003	0.112	0.018	0.099	4	0.5	-27.4	-9.3
SC	NL070710B	07/07/10	14.27	6.40	0.226	0.102	0.015	0.031	0.30	0.007	0.032	0.020	0.039	23			-7.0
SC	NL072010B	07/20/10	18.07	6.93	0.097	0.035	0.014	0.021	0.19	0.007	0.028	0.012	0.033	1	2.1		-8.9
SC	NL080310B	08/03/10	17.06	7.47	0.167	0.049	0.015	0.024		0.007	0.029	0.015	0.036		1.3		-8.4
SC	NL081710B	08/17/10	16.12	7.07	0.225	0.060	0.017	0.031	0.47	0.007	0.031	0.019	0.035	2	0.2		-8.2
SC	NL083110B	08/31/10	16.85	7.31	0.193	0.060	0.014	0.032		0.006	0.034	0.017	0.042		0.2	-27.1	-7.6
SC	NL091410B	09/14/10	15.95	7.65	0.147	0.039	0.014	0.017	0.37	0.006	0.041	0.027	0.038	13	1.1	-26.4	-7.3
SC	NL092810B	09/28/10	15.50	8.03	0.177	0.049	0.013	0.033	0.38	0.002	0.031	0.011	0.035	1	0.9		-7.5
SC	NL101210B	10/12/10	14.14	7.69	0.200	0.049	0.013	0.031	0.45	0.003	0.032	0.016	0.038	3	0.5		-6.3
SC	NL102610B	10/26/10	13.53	7.49	0.119	0.033	0.027	0.021	0.31	0.002	0.034	0.024	0.042	13	2.5		-7.7
SC	NL110910B	11/09/10	11.89	7.11	0.127	0.032	0.016	0.026		0.002	0.025	0.006	0.039		1.1	-26.5	-6.7
SC	NL112310B	11/23/10	11.14	7.47	0.064	0.035	0.024	0.023	0.27	0.002	0.022	0.004	0.039	21	3.0	-28.1	-9.4
SC	NL120710B	12/07/10			0.071	0.042	0.012	0.023	0.21	0.003	0.020	0.004	0.047	12	0.7		-7.7
SC	NL122110B	12/21/10	5.05	7.08	0.073	0.042	0.011	0.021	0.13	0.001	0.021	0.006	0.056	2	0.7		-8.2
SC	NL010411B	01/04/11	4.97	6.97	0.069	0.045	0.011	0.025	0.81	0.001	0.017	0.002	0.054	56	0.9		-8.0
SC	NL011811B	01/18/11	3.19	7.19	0.072	0.045	0.010	0.024	0.33	0.001	0.020	0.001	0.051	25	0.7	-26.6	-8.1
SC	NL020811B	02/08/11	3.84	7.34	0.071	0.047	0.011	0.023	0.33	0.002	0.017	0.011	0.052	26	0.7		-8.0
SB	LF051311B	05/13/11	13.84	6.94	6.849	0.706	0.034	1.036	2.70	0.017	0.988	0.003	3.518	21			-5.7
BH	LF051511D	05/15/11	13.09	7.13	3.602	0.486	0.029	0.798	2.10	0.016	0.348	0.015	2.246	13			-4.5
BC1	LF051511A	05/15/11	15.20	6.59	6.084	1.536	0.113	4.794	4.11	0.021	1.893	0.000	4.302	16			-5.6
BCA	LF012012B	01/20/12	12.50	8.26	0.970	0.148			2.17				0.052	1			-11.7
TC	LF012012C	01/20/12	12.20	7.97	0.798	0.086			1.84				0.135	9			-13.1
CT	LF012012D	01/20/12	12.50	7.64	1.180	0.156			1.66				0.687	6			-11.4
SS	LF012012E	01/20/12	10.80	7.93	0.571	0.060			1.22				0.125	8			-8.7
HB	LF012012F	01/20/12	11.70	7.66	1.170	0.092			2.52				0.073	3			-12.9
SSS	LF012012G	01/20/12	11.30	7.80	0.535	0.116			1.74				0.062	18			-11.2
SCS	LF012012H	01/20/12	12.20	7.83	0.621	0.060			1.34				0.062	4			-11.3
DH1	LF012012I	01/20/12	10.90	7.93	0.551	0.052			1.19				0.187	13			-10.6
DH2	LF012012J	01/20/12	10.80	7.90	0.607	0.056			1.04				0.198	4			-10.6
SB	LF012012K	01/20/12	13.80	7.16	6.679	0.240			3.27				6.870	10			-10.7
OC3	LF012012L	01/20/12	13.40	7.48	8.176	0.336			4.00				7.911	8			-8.9
DC	LF012012M	01/20/12	6.90	7.31	7.257	1.219			3.92				8.119	9			-9.3
LH	LF012012O	01/20/12	13.80	8.22	1.521	0.140			2.98				0.094	2			-12.2

from the fraction of inorganic carbon in the solid residue. Secondary dehydration provided organic resin for isotopic analysis.

Measurements of the stable isotopes of carbon were conducted at the Stable Isotope Laboratory at the University of South Florida. For $\delta^{13}C_{DIC}$, 12 mL borosilicate glass vials with septa were filled with 1 mL of 85% phosphoric acid. After a flush of helium gas, 0.2 mL of sample was introduced into the vial with a syringe. The CO_2 produced in the reaction between the acid and the sample DIC was analyzed using a Thermo-Finnigan IRMS attached to a Gas Bench II. For $\delta^{13}C_{DOC}$, weighed masses of organic resin were loaded into tin capsules and combusted in an Elemental Analyzer. The CO_2 produced in the combustion was analyzed in the IRMS. Isotopic values were compared to the VPDB standard using simultaneous measurements from reference samples of Carrara marble and NBS 18 standards for $\delta^{13}C_{DIC}$ and Fergie-CN for $\delta^{13}C_{DOC}$. Measurements of $\delta^{13}C_{DIC}$ and $\delta^{13}C_{DOC}$ are accurate to within ±0.1‰.

ANALYSIS OF ANALYTICAL RESULTS

The saturation index with respect to calcite and gypsum and the calcite saturation ratio for each sample were computed using the Debye Hückle relationship to compute molar activities of ionic species as summarized by Ford and Williams (2007) and White (1988) for the carbonate equilibrium reactions. Additionally for each sample, the partial pressure of CO_2 in solution, PCO_2, was computed using the temperature-dependent equilibrium equations for pK_{CO2}, pK_1, pK_2, and pK_c summarized in Ford and Williams (2007, p. 48) and derived from Garrels and Christ (1965) and Plummer and Blusenberg (1982). Using Henry' Law, the equivalent molar concentration of CO_2 in solution was computed from PCO_2. The sum of the molar concentrations of CO_2 and HCO_3^{1-} in solution is a measure of the total DIC in solution. Summaries of computed geochemical values are provided in Tab. 2.

Tab. 2. Summary of analytical data.

Site	Sample Name	Date	SIcal	C/Cs	SIgyp	PCO_2 atm	CO_2 mmol/L	DIC mmol/L
SS	NL070710A	07/07/10	0.06	0.99	-2.65	9.86E-04	4.72E-05	1.653
SS	NL072010A	07/20/10	-0.90	0.45	-2.75	6.59E-03	3.18E-04	1.828
SS	NL080310A	08/03/10	-0.06	0.90	-2.65	1.52E-03	6.89E-05	1.939
SS	NL081710A	08/17/10	0.01	0.95	-2.73	2.57E-03	1.20E-04	2.510
SS	NL083110A	08/31//10						
SS	NL091410A	09/14/10	-0.31	0.73	--2.61	3.88E-03	1.75E-04	2.265
SS	NL092810A	09/28/10						
SS	NL101210A	10/12/10	0.27	1.18	-2.57	1.70E-03	7.79E-05	2.688
SS	NL102610A	10/26/10	0.28	1.19	-2.46	1.56E-03	7.19E-05	2.592
SS	NL110910A	11/09/10						
SS	NL112310A	11/23/10	-0.17	0.83	-2.77	1.70E-03	8.30E-05	1.913
SS	NL120710A	12/07/10						
SS	NL122110A	12/21/10	-0.02	0.93	-2.77	2.34E-04	1.20E-05	1.002
SS	NL010411A	01/04/11	-0.68	0.55	-2.86	3.09E-03	1.60E-04	1.930
SS	NL011811A	01/18/11	-0.44	0.67	-2.82	1.34E-03	6.84E-05	1.458
SS	NL020811A	02/08/11						
SC	NL070710B	07/07/10	-2.85	0.10	-3.59	6.57E-03	3.02E-04	0.602
SC	NL072010B	07/20/10	-2.86	0.09	-3.99	1.30E-03	5.35E-05	0.243
SC	NL080310B	08/03/10						
SC	NL081710B	08/17/10	-1.99	0.19	-3.64	2.25E-03	9.80E-05	0.568
SC	NL083110B	08/31/10						
SC	NL091410B	09/14/10	-1.68	0.24	-3.77	4.67E-04	2.04E-05	0.390
SC	NL092810B	09/28/10	-1.22	0.36	-3.73	1.99E-04	8.80E-06	0.389
SC	NL101210B	10/12/10	-1.43	0.30	-3.65	5.06E-04	2.33E-05	0.473
SC	NL102610B	10/26/10	-2.01	0.19	-3.81	5.51E-04	2.58E-05	0.336
SC	NL110910B	11/09/10						
SC	NL112310B	11/23/10	-2.35	0.14	-4.11	4.91E-04	2.47E-05	0.295
SC	NL120710B	12/07/10						
SC	NL122110B	12/21/10	-3.00	0.09	-3.88	5.43E-04	3.29E-05	0.163
SC	NL010411B	01/04/11	-2.36	0.14	-3.95	4.33E-03	2.63E-04	1.073
SC	NL011811B	01/18/11	-2.50	0.13	-3.93	1.05E-03	6.73E-05	0.397
SC	NL020811B	02/08/11	-2.36	0.14	-3.94	7.47E-04	4.70E-05	0.377
SB	LF051311B	05/13/11	-0.11	0.87	-0.53	1.51E-02	7.03E-04	3.403
BH	LF051511D	05/15/11	-0.25	0.78	-0.91	7.76E-03	3.69E-04	2.469
BC1	LF051511A	05/1511	-0.31	0.74	-0.54	5.17E-02	2.31E-03	6.420
BCA	LF0120312B	01/20/12	0.44	1.35	-2.99	6.25E-04	3.02E-05	2.200
TC	LF0120312C	01/20/12	0.01	0.95	-2.59	1.03E-03	5.04E-05	1.890
CT	LF0120312D	01/20/12	-0.23	0.79	-1.76	1.97E-03	9.53E-05	1.755
SS	LF0120312E	01/20/12	-0.34	0.72	-2.74	7.46E-04	3.79E-05	1.258
HB	LF0120312F	01/20/12	-0.02	0.94	-2.72	2.85E-03	1.41E-04	2.661
SSS	LF0120312G	01/20/12	-0.35	0.71	-3.07	1.44E-03	7.22E-05	1.812
SCS	LF0120312H	01/20/12	-0.37	0.71	-3.00	1.05E-03	5.11E-05	1.391
DH1	LF0120312I	01/20/12	-0.37	0.71	-2.58	7.28E-04	3.69E-05	1.227
DH2	LF0120312J	01/20/12	-0.41	0.68	-2.51	6.80E-04	3.46E-05	1.075
SB	LF0120312K	01/20/12	0.16	1.08	-0.29	1.09E-02	5.08E-04	3.778
OC3	LF0120312L	01/20/12	0.63	1.59	-0.18	6.28E-03	2.96E-04	4.296
DC	LF0120312M	01/20/12	0.40	1.33	-0.22	8.48E-03	4.85E-04	4.405
LH	LF0120312O	01/20/12	0.71	1.68	-2.52	9.43E-04	4.39E-05	3.024

VARIATION OF CARBON IN KARST AQUIFERS

Most generally, the results of this study reveal the blend of dissolved carbon that is transmitted though the largely epigene karst of the Cumberland Plateau. These data further reveal information on the source and timing of carbon transport. As a baseline for further research, the data characterize the magnitude of carbon flux in present conditions. Since rates of chemical weathering are sensitive to environmental and climate conditions, reference studies as this provide one important regional context to help understand the potential impacts of changes in land use (Zhang 2011) and atmospheric CO_2 (Cao *et al.* 2012) upon temperature, precipitation, plant community structure, and resultant DOC and DIC in karst aquifers.

DOC AND $\delta^{13}C_{DOC}$

Values of DOC are within the expected range of karst waters as observed by Simon *et al.* (2007). Values at the aquifer input (SC) are consistently higher (average and standard deviation = 1.11±0.82 mg/L) than at the aquifer output (SS) (average and standard deviation = 0.97±0.47 mg/L). This suggests a conversion of DOC into DIC between aquifer input and output that is at least in part due to microbial activity. DOC values at SC are particularly sensitive to discharge (Fig. 3). During August 2010 when dry conditions reduced the base flow at SC to less than 0.8 L/s, DOC levels were close to zero. In contrast, higher discharge conditions

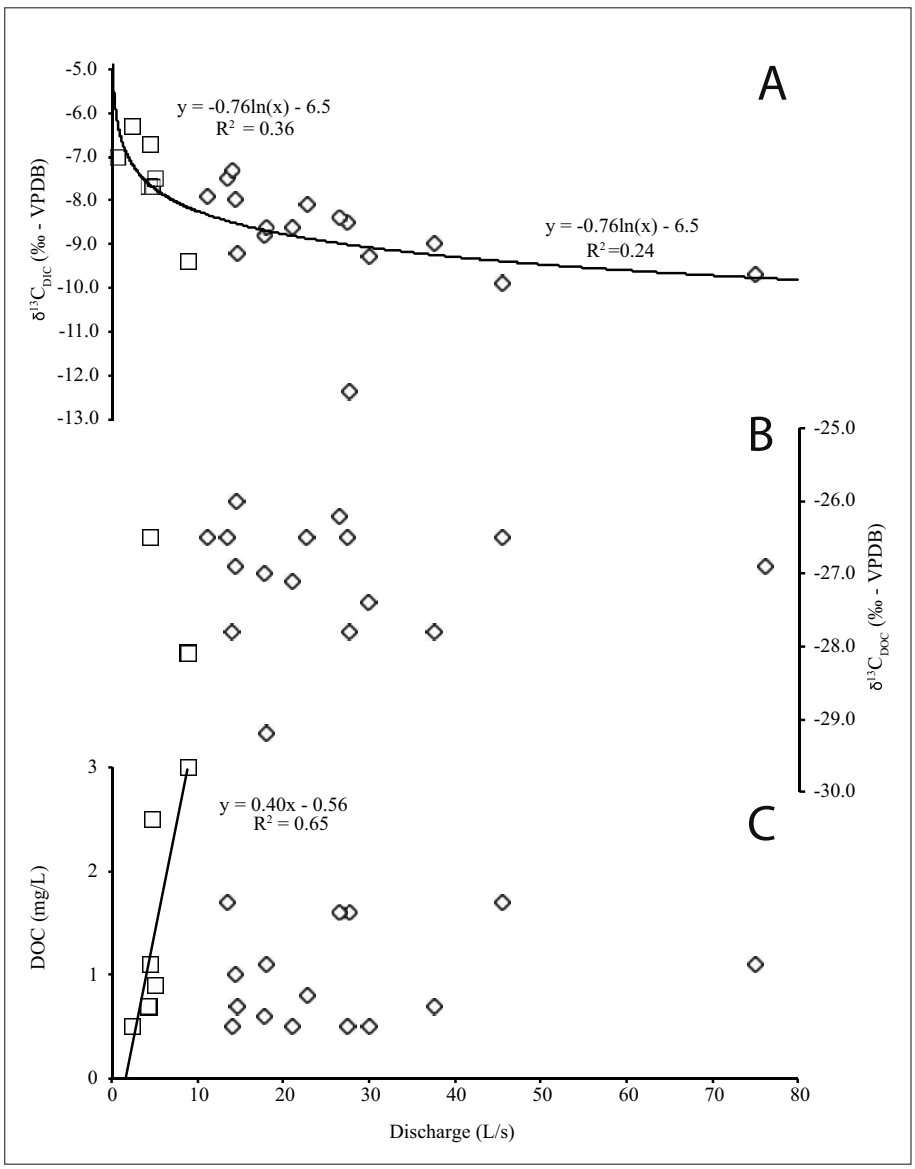

Fig. 3: Analytical measurements of A) $\delta^{13}C_{DIC}$, B) $\delta^{13}C_{DOC}$, and C) DOC compared against measured value of discharge with Stream Cave (SC) shown as open squares and Sandy Springs (SS) shown as open diamonds. A linear regression is shown for values of DOC at SC in panel C. Matched logarithmic regressions for values of $\delta^{13}C_{DIC}$ are shown for SC and SS in panel A.

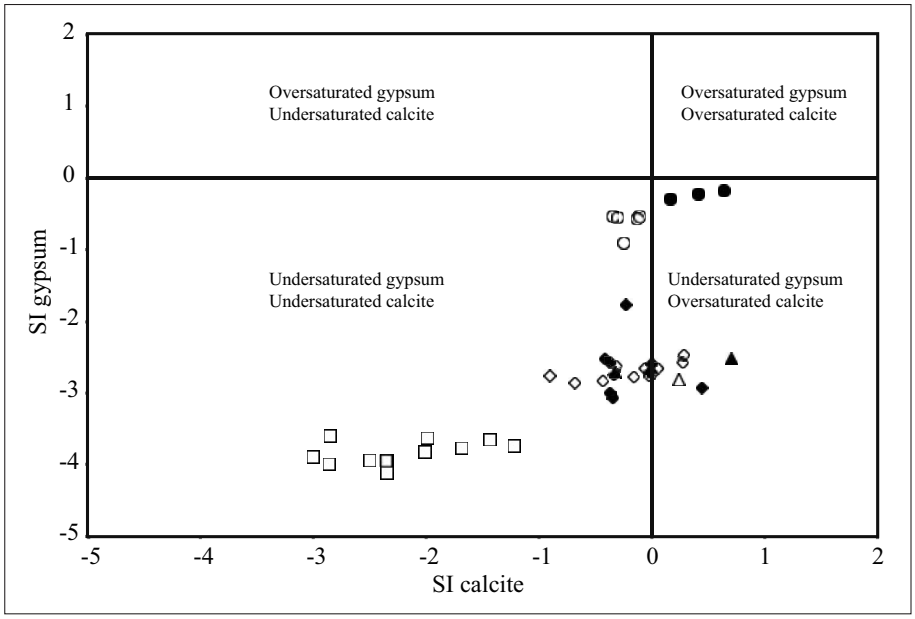

Fig. 4: Calculated values of saturation index for calcite (x-axis) and gypsum (y-axis) at Stream Cave (SC – open squares), Sandy Springs (SS – open diamonds), and sulfur seeps (open circles) from 2010–2011. Also shown are DIC measurements from 2012 samples including those from karst springs (filled diamonds), the tufa spring (filled triangle), and the sulfur seeps (filled circles). Undersaturated and oversaturated fields are identified.

in October and November 2010, combined with organic loading from falling deciduous leaves, produced DOC values up to 3 mg/L. No similar relationship between DOC and Q is visible at SS; however, similar timing of high and low values of DOC is clear from the time series data (Fig. 3).

Despite scatter, the contribution of C3-type vegetation is clearly demonstrated by the values of $\delta^{13}C_{DOC}$ observed at both SC and SS (average and standard deviation = -27.0±0.8‰). No relationship between $\delta^{13}C_{DOC}$ and Q is visible in Fig. 3, suggesting that the source of DOC does not shift either seasonally from agriculture or according to availability of water. This conforms to existing land use in the watersheds for both SC and SS, which are minimally impacted by human activities, being primarily woodland with a history of selected timber harvesting dating back to the early 1900s (Kay Koger, landowner – personal communication). The estimated population density for Redmond Creek is ~ 0.01 ha^{-1} and is a similar density for the larger Otter Creek watershed.

$\delta^{13}C_{DIC}$ AND DIC CONCENTRATION VERSUS DISCHARGE

$\delta^{13}C_{DIC}$ values from the Otter Creek watershed generally coincide with carbonic acid dissolution of limestone. The concentration of this DIC generally decreases with increasing Q. Data from SC and SS in 2010–2011 weakly suggest that $\delta^{13}C_{DIC}$ at the aquifer output is inversely proportional with discharge (Fig. 3) indicating that undersaturated waters during higher discharge conditions have excess soil-derived PCO_2 and contribute more depleted $\delta^{13}C_{DIC}$ values than during base flow conditions. Conversely, base flow conditions are more enriched in ^{13}C, with weak logarithmic regressions for SC and SS that approach -6.5‰ at a Q = 1 L/s (Fig. 3).

$\delta^{13}C_{DIC}$ values are somewhat dependent upon the DIC concentration at SC and SS, but not among the other sites in this dataset, including tufa springs and sulfur seeps (Fig. 5). DIC in the form of HCO_3^- dominates the water chemistry (Tab. 1 and 2). The concentration of DIC among all samples increases with calcite saturation and, on average, exceeds 2 mmol/L in saturated waters (Fig. 5). Along the flowpath between SC and SS, DIC in CO_2 form is converted to HCO_3^- via the reaction in Equation 1. Careful inspection of data in Tab. 2 demonstrates greater CO_2 concentration at SS when compared to SC (average and standard deviations = $1.1x10^{-4}$±$0.85x10^{-4}$ and $0.8x10^{-4}$±$0.98x10^{-4}$, respectively); however, at SC the CO_2 comprises a greater fraction of the DIC in the sample (Fig. 5).

$\delta^{13}C_{DIC}$ VERSUS CALCITE SATURATION

Walden (1999), during an investigation of groundwater from the Redmond Creek karst aquifer, used ratios of $^{87}Sr/^{86}Sr$ to differentiate between conduit and diffuse flow. Her results expectedly found a trend toward values similar to the host limestone along the aquifer flow path. Following this logic, values of SI and C/Cs should in theory approach, or even exceed, saturation along that same flowpath. Data from Tab. 2 demonstrate that this is likely the case with values of SI at SC (average and standard deviation = -2.62±0.59), an input to the Redmond Creek aquifer, consistently lower than at SS (average and standard deviation = -0.56±0.39), the primary output for the Redmond Creek aquifer.

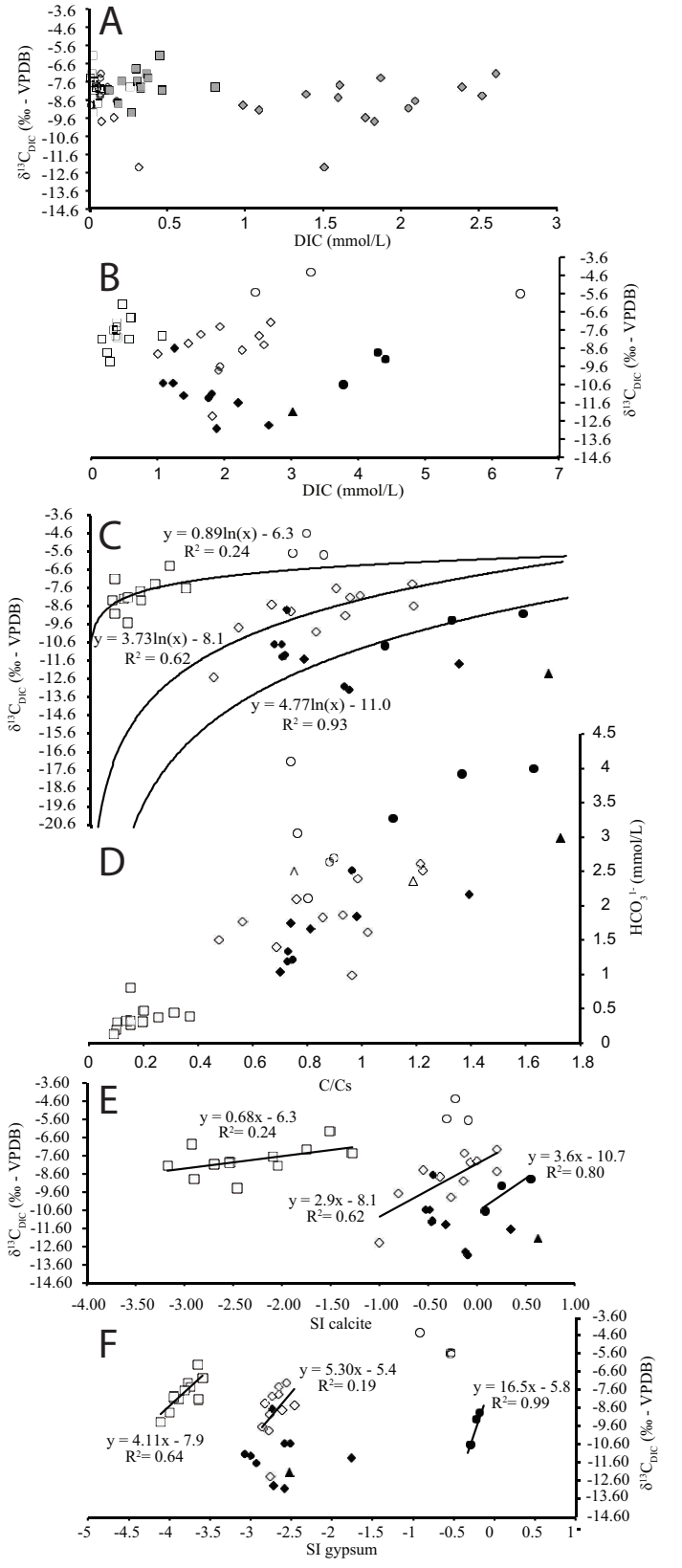

Correspondingly, values of $\delta^{13}C_{DIC}$ should increasingly reflect DIC derived from the bedrock. With an approximated shift of +6.4‰ from CO_2 in the soil to CO_2 in solution (Clark and Fritz 1997), water with C/Cs = 0 that is in equilibrium with soil CO_2 should have a $\delta^{13}C_{DIC}$ of -20.6‰. Theoretically, karst water with a SI = 0 or C/Cs = 1 would have a 50% blend of DIC from the soil and from the bedrock following *Equation 1.* Without prior knowledge of the bedrock end member, the value of $\delta^{13}C_{DIC}$ expected at saturation is unknown. However, the data from both SC and SS appear to converge at saturation to a $\delta^{13}C_{DIC}$ value of -6.3‰ and -8.1‰ for SC and SS, respectively (Fig. 5), which is similar to the values observed at base flow conditions in Section 5.3 (Fig. 3). Assuming that *Equation 1* is the only reaction pathway for producing DIC, these results would imply a bedrock source of +8.4‰ for SC and +5.8‰ for SS, considerably more enriched in ^{13}C than typical values for marine carbonates that are typically close to that of the VPBD standard (e.g., Hoefs 1997). Since $\delta^{13}C$ of carbonates may vary by several per mille, a comparative investigation of the $\delta^{13}C$ signal of bedrock is currently underway to quantify the additional enrichment, if present.

Fig. 5: Analytical measurements of dissolved inorganic carbon (DIC) at Stream Cave (SC – open squares), Sandy Springs (SS – open diamonds), and sulfur seeps (open circles) from 2010–2011. Also shown are DIC measurements from 2012 samples including those from karst springs (filled diamonds), the tufa spring (filled triangle), and the sulfur seeps (filled circles). From top to bottom: A) Values of $\delta^{13}C_{DIC}$ at SC and SS are compared against DIC concentration in the form of CO_2 (open symbols) and HCO^{3-} (gray-filled symbols). B) Values of $\delta^{13}C_{DIC}$ are compared against total DIC concentration. C) Values of $\delta^{13}C_{DIC}$ are compared against C/Cs with logarithmic regressions shown for data from SC and SS. D) DIC concentration in the form of HCO^{3-} are compared against the calcite saturation ratio (C/Cs). E) Values of $\delta^{13}C_{DIC}$ are compared against the saturation index with respect to calcite; linear regressions are shown for the data from SC and SS. F) Values of $\delta^{13}C_{DIC}$ are compared against the saturation index with respect to gypsum; linear regressions are shown for the data from SC and SS.

One possible source of additional $\delta^{13}C_{DIC}$ enrichment is evident in the data from the sulfur seeps. These sites are closer to saturation with respect to gypsum (Fig. 4). In 2011 these sites, despite high values of Ca^{2+} and HCO_3^- in solution (Tab. 1), are undersaturated with respect to calcite (Tab. 2). They are correspondingly enriched with respect to ^{13}C (Fig. 5). This implies additional enrichment in bedrock carbon without a corresponding additional contribution from PCO_2 from the soil. Such a process may be driven by the oxidation of dissolved sulfides, which can decrease the pH and drive additional carbonate dissolution via *Equation 2*. Interestingly, the 2012 data from the sulfur seeps reveal oversaturation with respect to calcite and decreased enrichment of ^{13}C. These samples were collected in higher discharge conditions during the winter months. They follow trends similar to SC and SS and converge on a value $\delta^{13}C_{DIC}$ of -11‰ at SI = 0 and C/Cs = 1 (Fig. 5). Collectively these data suggest the potential for lessened oxidation of reduced sulfur at the time of the 2012 samples.

The particular reason why the 2012 sulfur seep samples are more depleted in ^{13}C compared to the samples from SS, which are in turn more depleted in ^{13}C than the samples from SC is unclear. Logic suggests that the trend should be the opposite; the potential influence of *Equation 2* upon $\delta^{13}C_{DIC}$ should increase at sites with known influence of sulfur-rich brines, which is certainly the case the sulfur seeps and observed to a lesser degree at sites within the cave that contributes to SS. One possible mechanism that could generate the trends in Fig. 5 is that the average bedrock $\delta^{13}C_{DIC}$ may vary by several per mille within the contributing watershed for each site. A second possibility is the potential for the oxidation of pyrite within the bedrock within the watershed of SC, known to be present in significant quantities in the Bangor Limestone and the organic-rich shale and coal that overlie the Bangor. A third possibility is the potential for methanogenesis within the deeper flow systems that contribute some percentage of flow to SS and the sulfur seeps where reduction of organics may lead to depleted values of $\delta^{13}C_{DIC}$. Finally, the samples from SC, which represent waters that have limited interaction with bedrock, may simply not be in equilibrium with soil CO_2. Each of the postulates remains untested at this time.

Of the remaining samples during 2012 from all other sites, the values of $\delta^{13}C_{DIC}$ are equal to, or more depleted than those observed at SS in 2010–2011 (Fig. 5). Five of those sites, CT, SSS, SCS, DH1, DH2, are clustered and similar in range to the data from SS. These five springs have similar physical characteristics (stratigraphic position, discharge, etc.) to SS. Four other sites, BCA, TC, HB, and LH, are depleted in ^{13}C compared to the other samples at the same calcite saturation. These springs may collect waters from aquifers that have somewhat different bedrock isotope composition than SS or each other. The sample from LH is significantly oversaturated with respect to calcite and is an active tufa spring. Fractionation of the heavier isotope during $CaCO_3$ precipitation combined with degassing of CO_2 enriched in the lighter isotope potentially drives this sample toward depletion. The remaining three depleted sites may also experience similar fractionation from degassing and calcite precipitation to varying degrees and underscores the complexity of interpreting a limited number of $\delta^{13}C_{DIC}$ values from a site.

CONCLUSIONS

In the Otter Creek watershed of the Cumberland Plateau of Kentucky, USA, the concentration of dissolved organic carbon is less than 3 mg/L, and in the case of some sites is inversely proportional to discharge. C3 vegetation is the source of this DOC, with an average $\delta^{13}C_{DOC}$ of −27‰. DIC concentrations that may exceed 4 mmol/L are inversely proportional to discharge and directly proportional to the saturation of the aqueous solution with respect to calcite and gypsum at some sites. Values of $\delta^{13}C_{DIC}$ reflect soil and bedrock sources and conform to measurements expected from the carbonate equilibrium reactions. Increasing enrichment of ^{13}C at two sites in this study proceeds with increased saturation of groundwater with respect to calcite. Sulfur seeps follow this same trend at higher base flow conditions. These same sulfur seeps are enriched in ^{13}C at low flow, but undersaturated, thus suggesting that the oxidation of reduced sulfur may enrich these sties in bedrock DIC. Other locations appear to follow independent DIC pathways. Some sites, such as tufa springs may have depleted $\delta^{13}C_{DIC}$ from CO_2 degassing and calcite precipitation.

ACKNOWLEDGEMENTS

The author acknowledges the major contributions by Bill Walden, Chasity Stinson, and Nick Lawhon during sample collection as well as the conversations, hospitality, and access provided by landowners Tim Pyles and Kay Koger and cavers Rick Gordon, Deb Moore, Harry Gopel, and Eric Weaver. Finally, the author appreciates the collaborations with Jonathan Wynn and Bogdan Onac at the USF Stable Isotope Laboratory. Funding for this work was provided by a WKU Provost Incentive grant, a WKU start-up index, and a Ball State University start-up package. Welcome comments from two anonymous reviewers greatly improved the flow and content of this manuscript.

REFERENCES

Abbott, W.R., 1921: Oil Field Map–Wayne and Clinton Counties, Kentucky.

Anthony, D.M. & D.E. Granger, 2004: A Late Tertiary origin for multilevel caves along the western escarpment of the Cumberland Plateau, Tennessee and Kentucky, established by cosmogenic ^{26}Al and ^{10}Be.- Journal of Cave and Karst Studies, 66, 2, 46–55.

Berner, R.A., Lasaga, A.C. & R.M. Garrels, 1983: The carbonate–silicate cycle and its effect on atmospheric carbon dioxide over the past 100 million years.- American Journal of Science, 284, 641–683.

Clark, I.D. & P. Fritz, 1997: *Environmental Isotopes in Hydrogeology.*- Lewis Publishers, Boca Raton, 328 pp.

Crawford, N.C., 1984: Karst landform development along the Cumberland Plateau Escarpment of Tennessee. In: RG LeFleur (ed.), *Groundwater as a geomorphic agent.* Boston, Allen and Unwin, Inc., pp. 294–338.

Dugan, C.R., Florea, L.J. & W.D. Walden, 2012: A Geochemical Investigation of Springs within the Otter Creek watershed: Wayne County, Southeastern Kentucky.- Geological Society of America Abstracts with Programs, 44, 4, 26.

Ehleringer, J.R., Buchmann, N. & L.B. Flanagan, 2000: Carbon isotope ratios in belowground carbon cycle processes.- Ecological Applications, 10, 2, 412–422.

Ettensohn, F.R., Rice C.R., Dever, G.R. Jr. & D.R. Chesnut, 1984: Slade and Paragon Formations; New stratigraphic nomenclature for Mississippian rocks along the Cumberland Escarpment in Kentucky.- U.S. Geological Survey Bulletin 1605–B, 37 pp.

Florea, L.J.l., 2013: Selective recharge and isotopic composition of shallow groundwater within temperate, epigenic carbonate aquifers. *Journal of Hydrology 489:* 201–213. doi 10.1016/j.jhydrol.2013.03.008

Florea, L.J., 2013a: Investigations into the Potential for Hypogene Speleogenesis in the Cumberland Plateau of Southeast Kentucky, U.S.A. In, *Proceedings of the 16th International Congress of Speleology, Brno, Czeck Republic, July 2013,* pp. 356–361.

Ford, D.C. & P. Williams, 2007: *Karst Hydrogeology and Geomorphology.*- John Wiley & Sons, 562 pp.

Garrels, R.M. & C.M. Christ, 1965: *Solutions, Minerals, and Equillibria.* Harpers' Geoscience Series. Harper and Row, New York. 450 pp.

Hill, C.A., 1990: Sulfuric acid speleogenesis of Carlsbad Cavern and its relationship to hydrocarbons, Delaware Basin, New Mexico and Texas.- American Association of Petroleum Geologists Bulletin, 74, 11, 1685–1694.

Hoefs, J., 1997: *Stable isotope geochemistry.;* 4th Ed., Springer, New York, 200 pp.

Cao, J.H., Yuan, D.X., Groves, C., Huang, F., Huang H. & Q. Lu, 2012: Carbon fluxes and sinks: The consumption of atmospheric and soil CO_2 by carbonate rock dissolution.- Acta Geologica Sinica, 86, 963–972.

Kendall, C. & E.A. Caldwell, 1998: Fundamentals of Isotope Geochemistry. In: Kendall, C. & J. J. McDonnell, (eds.), *Isotope Tracers in Catchment Hydrology Elsevier Science B.V.,* Amsterdam, pp. 51–86.

Marlier, J.F. & M.H. O'Leary, 1984: Carbon kinetic isotope effects on the hydration of carbon dioxide and the dehydration of bicarbonate ion.- Journal of the American Chemical Society, 106, 5054–5057.

Palmer, A.N., 1991: Origin and morphology of limestone caves.- Geological Society of America Bulletin, 103, 1–21.

Plummer, L. & N.E. Busenberg, 1982: The Solubilities of calcite, aragonite and vaterite in CO_2 - H_2O solutions between 0 and 90°C, and an evaluation of the aqueous model for the system $CaCO_3$ - CO_2 - H_2O.- Geochimica et Geochimica Acta, 46, 1011– 1040.

Rantz, S.E., 1982: Measurement and computation of streamflow, Volume 1, Measurement of stage and discharge.- United States Geological Survey Water Supply Paper 2175, 284 p.

Sasowsky, I.D. & W.B. White, 1994: The role of stress release fracturing in the development of cavernous porosity in carbonate aquifers.- Water Resources Research, 30, 12, 3523–3530.

Schlesinger, W.H., 1997: *Biogeochemistry: An Analysis of Global Change*.- Academic Press, San Diego, 443 pp.

Simon, K.S., Pipan, T. & D.C. Culver, 2007: A conceptual model of the flow and distribution of organic carbon in caves.- Journal of Cave and Karst Studies, 69, 2, 279–284.

Simpson, L.C. & L.J. Florea, 2009: The Cumberland Plateau of Eastern Kentucky.- In: Palmer, A.N. & MV Palmer (eds.), Caves and Karst of America. National Speleological Society, pp. 70–79.

Walden, K., 1999: *Strontium isotopes in Redmond Creek Cave, Monticello, Kentucky.*- Honors Thesis, Ohio State University, 66 p.

Walden, W.D., Walden, K.M. & L.J. Florea, 2007: The Caves and Karst of Redmond Creek, Wayne County, Kentucky.- National Speleological Society Convention Program Guide, p. 107.

White, W.B., 1988: *Geomorphology and Hydrology of Karst Terrains*. New York, Oxford University Press, 464 pp.

Zhang, C., 2011: Carbonate rock dissolution rates in different landuses and their carbon sink effect.- Chinese Science Bulletin, doi: 10.1007/s11434–011 –4404–4.